Proceedings World Geothermal Congress 2026
Calgary, Canada, June 8 – 11, 2026

Heli-borne Data Combined Curie Point Depth Analysis For Assessment Of Supercritical Carbon Recycle CO2 Geothermal Power Generation

Shunsuke Akazawa[1*], Yasukuni Okubo[1], Shoichi Yamano[1], Takumi Kimoto[1], Kazumi Osato[1], Amane Terai[2]
Geothermal Energy Research & Development Co., Ltd. [1*], JOGMEC[2]
akazawa@gerd.co.jp

Keywords: Curie point depth, Japanese Islands, supercritical CO2, geothermal, heli-borne magnetic

INTRODUCTION

Since 2011, the Japanese government has begun a policy to enhance renewable energy. This includes the project of supercritical carbon (SC-CO2) recycle CO2 geothermal power generation launched in fiscal year 2021. This concept was proposed by Brown (2000) based on the experience of the very extensive hot dry rock research conducted by Los Alamos National Laboratory at Fenton Hill. To extract energy from dry rocks at depth, enhanced geothermal systems (EGS) are currently being developed.

As a result of various drilling surveys in Japan, many geothermal areas have been discovered, including areas where high temperatures have been confirmed at depth but no signs of hot water have been found. These areas are thought to be hot dry rock areas. Japan Organization for Metals and Energy Security (JOGMEC) launched the project of geothermal system using SC-CO2 in 2021 in order to develop such hot dry rock areas. This is a technology to generate electricity using SC-CO2 instead of water.

In the USA, a map of geothermal energy potential of hot dry rock across the USA (National Renewable Energy Laboratory, 2018) has been published. Following the achievement, in the overall system design, in order to reveal the geothermal structure of the Japanese islands and to estimate the potential for SC-CO2 geothermal power generation, we conducted Curie point depth (CPD) analysis.

Ishihara and Uchida (2021) published East/Southeast Asia magnetic anomaly map (3rd edition) at 2-minute intervals (we call it “IshiharaV3” hereafter). The data over land areas are air-borne (AB) data. Using the AB data, Okubo et al. (2023) calculated CPDs of the Japanese Islands by the method of Bouligand et al. (2009). We call the CPD “IshiCPD” hereafter.

A feature of the method of Bouligand et. al. (2009) is that the parameters are estimated using all data in the frequency range determined by a window size and a data interval. Okubo et al (2023) used the data at 3 km interval. Testing several window sizes, Okubo et al (2023) selected 50 km for the window size (Akazawa et al., 2025). The results range 6-9 km below sea level (BSL) in volcanic areas and are deeper than 9 km BSL in non-volcanic areas. Comparison between IshiCPDs and drillhole data shows that CPDs miss to extract the local high anomalies. The reason is that the IshiCPD corresponds to the average value of the 50 km square area (Okubo et al., 2025). Therefore, in order to improve the spatial resolution, we attempt to reduce the window size.

JOGMEC is conducting helicopter-borne (HB) magnetic surveys at several geothermal fields with short flight intervals. Here, taking the Hachimantai geothermal field (GF) in the Tohoku arc as a study area, we used the HB magnetic data to improve the spatial resolution of CPD analysis. Furthermore, the results were integrated with the depth to temperature (DtT) data of drillholes to construct a 3D geothermal structural model that will be useful for assessment of SC-CO2 power generation.

1 AB and HB Magnetic Data Compilation

The study area, the Hachimantai GF, is located in the Tohoku arc. Volcanoes of Akita-Yakeyama, Hachimantai, Iwate volcano, and Akita-Komagatake are distributed there. In addition, the Kakkonda geothermal power plant (GP) (8.0MW), the Matsukawa GP (2.3MW), the Matsuo-Hachimantai GP (0.7MW), the Onuma GP (1.0MW), and the Sumikawa GP (5.0MW) are in operation.

Figure 1 shows the IshiCPD map of the Hachimantai GF. The CPDs are about 7.5km BSL at the Kakkonda GP, 7km BSL at the Matsukawa GP, 7.8km BSL at the Matsuo-Hachimantai GP, and 8km BSL at the Onuma and the Sumikawa GPs.

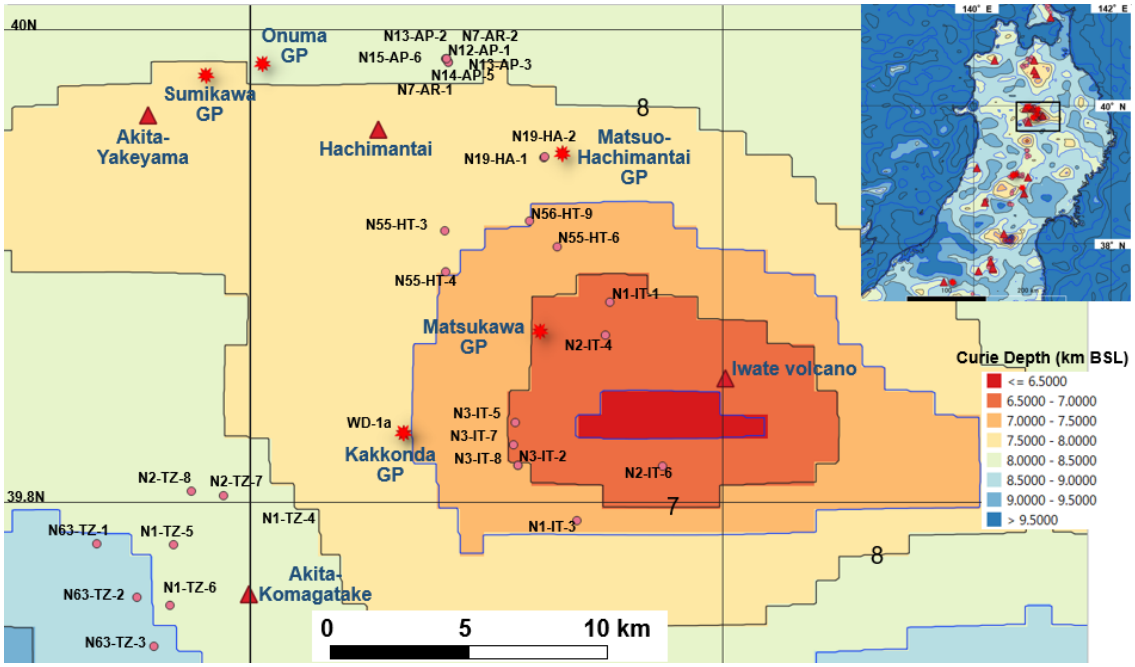


Figure 1: IshiCPD contour map of the Hachimantai GF calculated using IshiharaV3. Right-top figure shows IshiCPD map of Tohoku and black rectangular in the figure indicates location of Hachimantai GF.

JOGMEC is conducting helicopter-borne (HB) magnetic surveys in the Hachimantai GF. The flight lines of the HB magnetic survey run in an east-west direction with an interval of 250 m (Figure 2). There are many places where helicopters could not fly, so there are many blank areas. Magnetic data from a sensor altitude of about 100 m was continued upward to altitude of 1500 m. The method used was that of Nakatsuka and Okuma (2009). The upward continued HB magnetic data was compiled with the IshiharaV3 at an altitude of 1500 m.

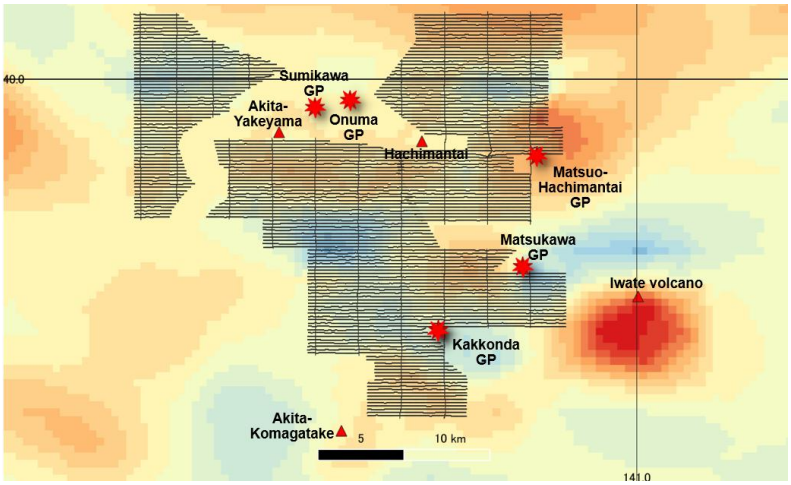


Figure 2: AB and HB combined magnetic map. Black lines denote flight tracks of HB survey.

The survey line interval for the IshiharaV3 magnetic data is 3-4 km. When data are converted to a grid interval smaller than 3 km, a spectrum could generate noise by interpolation in the range of wave numbers higher than π/3 (1/km). This causes an ill inversion. Therefore, Okubo et al. (2023) used a grid interval of 3 km for the IshiharaV3 magnetic data. Here, we created 2 km interval grid data of the AB and HB combined data for CPD analysis. Figure 2 shows the magnetic data, which includes short wavelength components not found in IshiharaV3.

2 CPD Analysis Method Applied to Magnetic Data

CPD analysis is widely used to understand geothermal structure by analyzing magnetic data. Since EMAG2, which is compiled from satellite, ship, and AB magnetic measurements (Maus et al., 2009) and covers globally at 2-minute intervals, was released as open data, CPD analysis has been applied in many regions. The results are used to understand regional geothermal structure and for geothermal resource assessment.

CPD analysis used here is based on spectral analysis of magnetic data. The theoretical power spectrum due to a slab of self-similar magnetization distribution is given by Maus and Dimri (1996). The power spectrum depends on three parameters, the top depth of the magnetized layer (Zt), the thickness of the magnetized layer (Dz), and the fractal coefficient β. CPD is simply calculated from Zt and Dz by the following formula.

$$\mathrm{CPD} = \mathrm{Zt} + \mathrm{Dz}$$

We used the Bayesian framework to determine the three parameters simultaneously. The algorithms were implemented within PyCurious, an open-source Python package.

Window size defines the low frequency range. The thickness of the magnetized layer (Dz) greatly affects the shape of radial power spectra. As Dz increases, changes appear at lower frequencies. It is necessary to enlarge the window size in order to accurately estimate the deep depth to the bottom of magnetized layer. So that window size is significant to estimate Dz.

Comparison between IshiCPDs and drillhole data in the Hachimantai GF shows that IshiCPDs miss to extract the local high anomalies. The reason is that the CPD corresponds to the average value of the 50 km square area which is the window size for CPD analysis (Okubo et al., 2025).

HB magnetic data contains short-wavelength components that reflect shallow structures. Therefore, to increase spatial resolution, the window size was changed from 50 km to 40 km, and the data interval was changed from 3 km to 2 km for the AB and HB combined magnetic data. Then Curie point analysis was performed. Reducing the window size and narrowing the data interval made the inversion more unstable. By trial and error with the initial values and parameters of probability function in the Bayesian framework, a stable solution was obtained.

Figure 3 shows CPDs calculated with a grid interval of 2 km of the AB and HB combined magnetic data and a window size of 40 km. We call it “HeliCPD” hereafter. The HeliCPDs are about 7km BSL at the Kakkonda GP, 6.5km BSL at the Matsukawa GP, 6.7km BSL at the Matsuo-Hachimantai GP, and 7km BSL at the Onuma and the Sumikawa GPs.

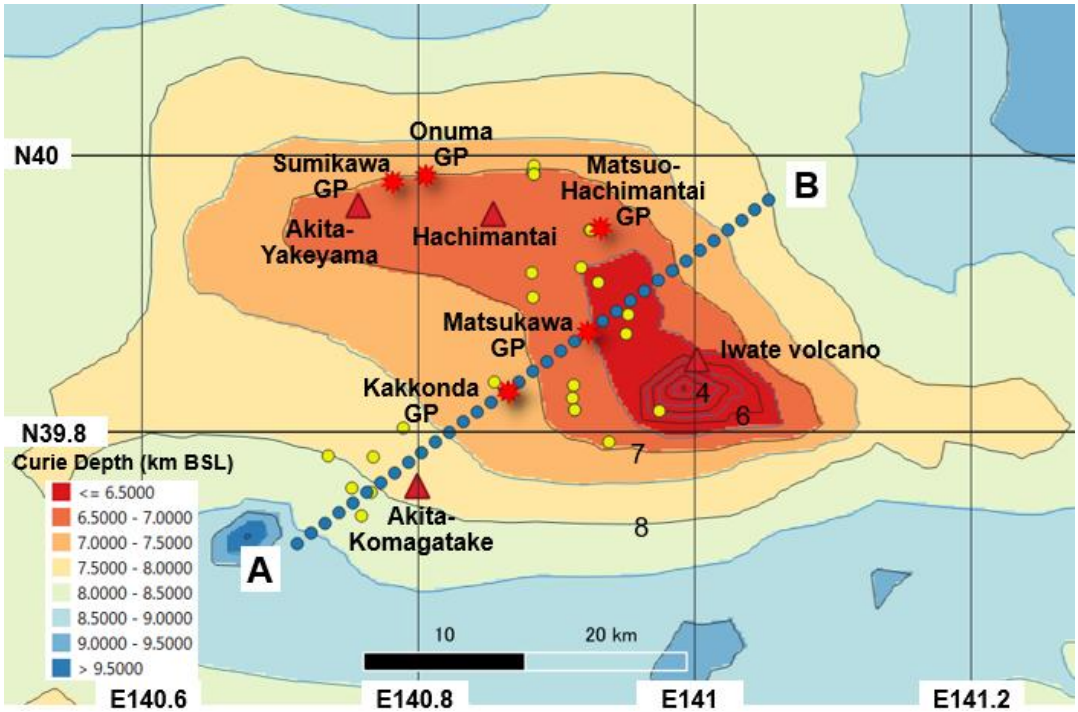


Figure 3: HeliCPD map of the Hachimantai GF calculated using AB and HB combined magnetic map. A-B line indicates profile line of Figure 4.

Figure 4 shows comparison of IshiCPDs and HeliCPDs crossing the Kakkonda and the Matsukawa GPs. The HeliCPDs are entirely shallower than the IshiCPDs. The differences between the two are a maximum of 1 km around the geothermal power plant where HB data are available, and about several hundred meters in the surrounding area. At the Onuma and the Sumikawa GPs, the HeliCPDs (Fig.3) is 1km shallower than IshiCPDs.

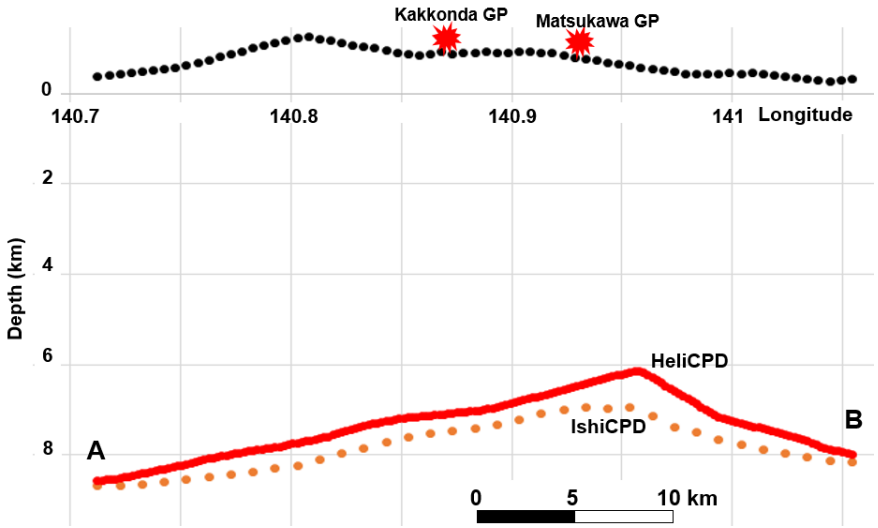


Figure 4: Profile of CPDs. Orange dots are IshiCPDs and red line is HeliCPDs. Location of profile is indicated in Figure 3.

3 3D Geothermal Structural Model and Discussions

Here, we estimate the geothermal structure at depth and evaluate the potential of SC-CO2 geothermal power generation by compilation of HeliCPDs and drillhole data.

Geothermal Database System compiled by JOGMEC shows a number of measurements of depth to temperature (DtT) curves of drillholes in volcanic areas. The data provide local observed geothermal structure of the Hachimantai GF. Figure 5 shows the locations of drillholes with volcanoes, geothermal power plants in the study area.

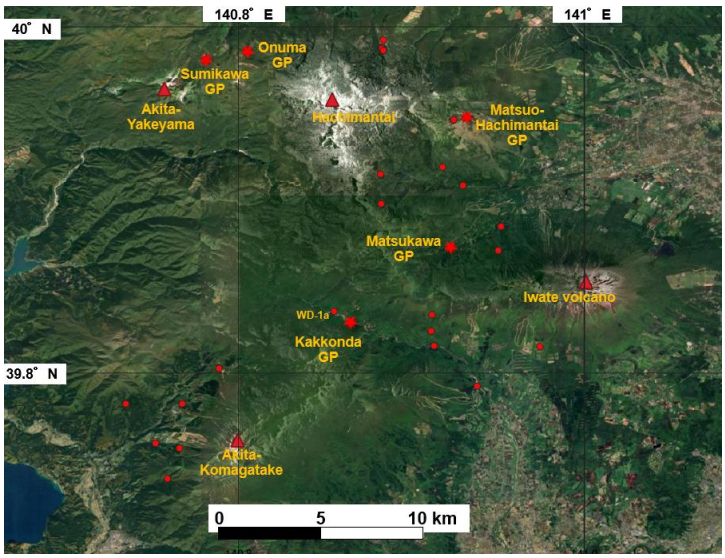


Figure 5: Locations of drillholes used (red circles), volcanoes (red triangles) and geothermal power plants (red stars) in the Hachimantai GF.

Leapfrog Geothermal modeling software ("Leapfrog", hereafter) has been developed to model and visualizes geothermal systems in three dimensions. The models are based on mathematical interpolation functions, and this provides a grid-free representation of the geological structure and numerical quantities such as temperature (Newson et al., 2012).

Drillhole data can extract local high temperature areas. However, the distribution is uneven and there are almost no data areas. In this approach, the initial step in integrating temperature model into Leapfrog is to assign dummy drillholes obtained by HeliCPDs shown in Figure 3 in order to cover the areas where there is no drillhole data. By assuming that the Curie point to be 580°C at CPD, 15°C at the surface and that the geothermal gradient is constant, we can make dummy DtT curves.

DtTs of drillhole are restricted at shallow parts ranging about 1000 m – 4000 m. Then we extrapolate the drillhole DtT curve below the bottom of hole by assuming that the geothermal gradient is constant from the bottom of hole to the deeper part.

The next is to integrate the extrapolated drillhole DtT curves and the dummy DtT curves by Leapfrog. In this way, we obtain a 3-D geothermal structural model for the entire Hachimantai GF. Figure 6 shows the contour of depth reaching CPD, 580℃ ("Leapfrog580" hereafter).

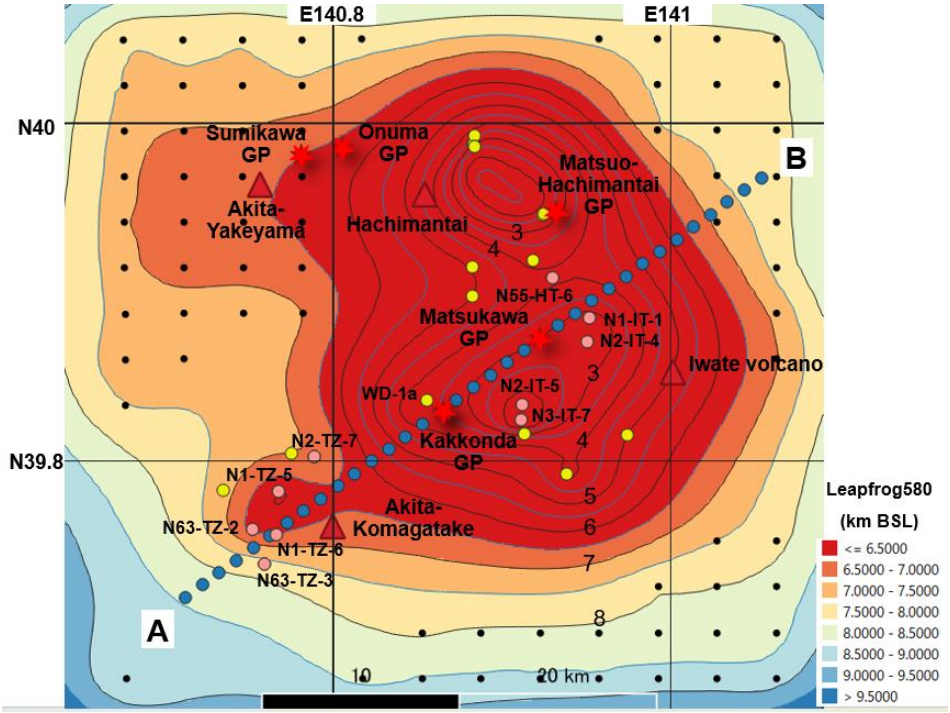


Figure 6: Contour of depth (km BSL) reaching CPD, 580℃. Contour interval is 0.5 km. Black dots denote locations of the dummy drillholes by HeliCPDs. Pink and yellow circles are locations of drillholes from the JOGMEC database. Drillholes data indicated by pink circles are plotted in Fig.7.

Figure 7 shows cross section of the 3D geothermal structural model across the Kakkonda and the Matsukawa GPs with integrating 374°C, 300°C, 200°C isotherms of the extrapolated DtT curves. The Leapfrog580 rises from 8 km BSL to 3 km BSL beneath the Kakkonda and the Matsukawa GPs, which is much shallower than HeliCPDs. The rise is a local geothermal anomaly with a horizontal width of about 20 km. The Kakkonda GP is located on the slope of the Leapfrog580 rise. The 374°C, 300°C, 200°C isotherms from the extrapolated DtT curves also show the local geothermal anomalies.

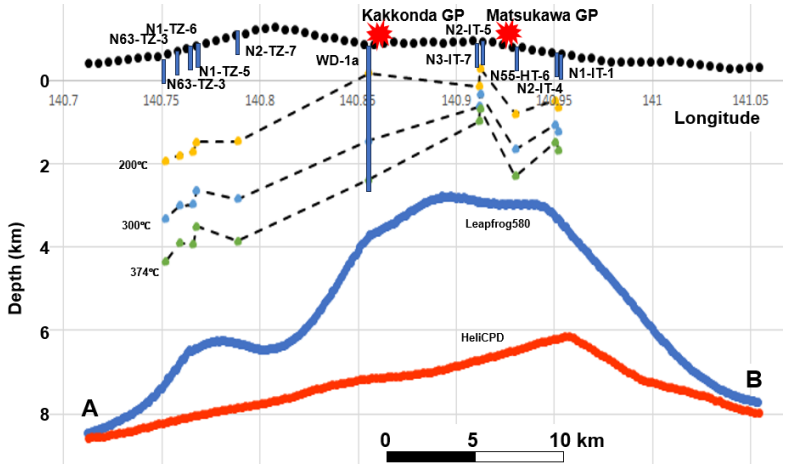


Figure 7: Cross section of 3D geothermal structural model across the Kakkonda and the Matsukawa GPs. Red line is HeliCPD and blue line is Leapfrog580. 374°C, 300°C, 200°C isotherms are from extrapolated drillhole DtT curves. Location of profile is indicated in Figure 6.

Figure 8 shows DtT curve of WD-1a (Ikeuchi et el., 1998). Drillhole of WD-1a, located at the Kakkonda GP, reached the Kakkonda granite at about 3000 m below the surface (Matsushima and Okubo, 2003). The temperature at the top of the granite was about 370°C. Temperature at the bottom of WD-1a, about 3km BSL, exceeds 500°C. The upper layer of the granite is a highly fractured volcanic rock layer. The DtT curves show that a hydrothermal convection type in the volcanic rock layer while a conductive type in the Kakkonda granitic layer. The temperature gradient is about 0.062 K/m in the volcanic layer, but increases to 0.2 K/m in the Kakkonda granite.

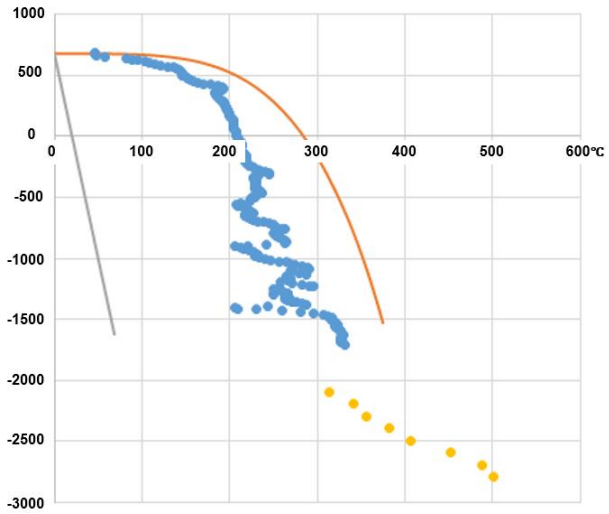


Figure 8: DtT curve (Blue and orange dots) of WD-1a (Ikeuchi et el., 1998). Orange curve is boiling curve of water. Purple line is the average geothermal gradient of the crust, 3K/100m.

The temperatures of 374°C, 300°C and 200°C at WD-1a in Figure 7 are the actual measured temperatures. The depth at which 580°C is reached, estimated from 0.2 K/m in the Kakkonda granite, is 3068 m BSL. This depth is significantly shallower than Leapfrog580.

WD-1a is the only drillhole that penetrates granite rocks and shows thermal conduction pattern with a high temperature gradient. We integrate the dummy drillhole data by CPDs, WD-1a and the surrounding drillholes into Leapfrog. As a result, the 3D geothermal structural model shows the average value of all data due to the averaging effect of the 3D interpolation. Accommodating all datasets, the model delineates high geothermal anomaly with a horizontal width of about 20 km at about several kilometers depth.

Taking all of this into consideration, we can envision a model in a geothermal area in which there is a single deep heat source and there are multiple hydrothermal convection systems above it with downward and upward flows in fracture dominated zone. The model is a good reference for a first stage assessment of SC-CO2 geothermal power generation.

4 Conclusions

Comparison between IshiCPDs and drillhole data in the Hachimantai GF shows that CPDs miss to extract the local high anomalies. The reason is that the IshiCPD corresponds to the average value of the 50 km square area which is the window size of Okubo et al. (2023).

We combined AB and HB data and created 2 km interval data. CPD analysis by the data with 40km window size shows shallower HeliCPDs reflecting the local high anomalies. We interpret that the HeliCPD analysis using the AB and HB combined magnetic data has improved the resolution.

The 3D geothermal structural model in the Hachimantai GF is made by inputting dummy drillhole data by HeliCPDs and the drillhole data into Leapfrog. As a result, the 3D geothermal structural model shows the average value of all data due to the averaging effect of the 3D interpolation. The model delineates high geothermal anomaly with a horizontal width of about 20 km at about several kilometers depth. This is a good reference for the assessment of SC-CO2 geothermal power generation.

Acknowledgement

This work is supported by a fund for the project “Carbon recycle CO2 geothermal power generation technology” from the Japan Organization for Metals and Energy Security (JOGMEC).

REFERENCES

Akazawa, S., Okubo, Y., Yamano, S., Osato, K. and Terai, A. (2025) Curie point depth map in Japan - Assessment in the Hatchobaru Geothermal Area-, Journal of the Geothermal Research Society of Japan.

Bouligand, C., Glen, J. M. G. and Blakely, R. J. (2009) Mapping Curie temperature depth in the western United States with a fractal model for crustal magnetization Claire, Journal of Geophysical Research, 114, B11104, doi:10.1029/2009JB006494.

Brown, D. W. (2000) A hot dry rock geothermal energy concept utilization supercritical CO2 instead of water, proceedings, 25thWorkshop on Geothermal Reservoir Engineering, Stanford University, 24-26.

Ikeuchi, K., Doi, N., Sakagawa, Y., Kamenosono, H. and Uchida, T. (1998) High temperature measurements in well WD-1A and thermal structure of the Kakkonda geothermal system, Japan, Geothermics, 27, 591-607.

Ishihara, T. and Uchida, T. (2021) Magnetic Anomaly Map of East and Southeast Asia, Revised Version (3rd Edition), Digital Geoscience Map P-3 Revised, Geological Survey of Japan.

Japan Oil, Gas and Metals National Corporation (JOGMEC) Geothermal Database System, https://geothermal-db-web.jogmec.go.jp/jogmec_db/map/php/login.php

Matsushima, J. and Okubo, Y. (2003) Rheological implications of the strong seismic reflector in the Kakkonda geothermal field, Japan, Tectonophysics, 371, 141 – 152.

Maus, S., Barckhausen, U., Berkenbosch, H., Bournas, N., Brozena, J., Childers, V., Dostaler, F., Fairhead, J.D., Finn, C., von Frese, R.R.B, Gaina, C., Golynsky, S., Kucks, R., Hai, Lu, Milligan, P., Mogren, S., Muller, R.D., Olesen, O., Pilkington, M., Saltus, R., Schreckenberger, B., Thebault, E. and Tontini, F.C. (2009). EMAG2: A 2-arc min resolution Earth Magnetic Anomaly Grid compiled from satellite, airborne, and marine magnetic measurements. Geochemistry, Geophysics, Geosystems, 10, Q08005.

Maus, S. and Dimri, V.P. (1996) Depth estimation from the scaling power spectrum of potential fields?, Geophys. J. Int., 124, 113-120.

Nakatsuka, T. and Okuma. (2009) Software system for Aeromagnetic data processing, Grid data manipulation, and Reduction and quantitative interpretation of magnetic anomaly data (2), GSJ Open-File Report, no. 519.

National Renewable Energy Laboratory (2018) Geothermal Resources of the United States.

Newson, J., Mannington, W., Sepulveda, F., Lane, R. G., Clearwater, E., & O'Sullivan, M. J. (2012). Application of 3D Modelling and Visualization Software To Reservoir Simulation: Leapfrog Geothermal and Tough2. Proceedings of Thirty Seventh Workshop on Geothermal Reservoir Engineering, 6.

Okubo, Y., Yamano, S., Akazawa, S., Osato, K. and Terai, A. (2025) Curie point depth analysis for assessment of supercritical carbon recycle CO2 geothermal power generation, Proceedings, 50th Workshop on Geothermal Reservoir Engineering Stanford University, Stanford.

Okubo, Y., Yamano, S., Takanashi, K., Akazawa, S., Osato, K. and Terai, A. (2023) Constraining the geotherm beneath the Japanese islands from Curie point depth analysis and comparison with seismicity and drillhole data in the Kakkonda geothermal field. Geothermics, 111, 102706.